SMM behaviour and magnetocaloric effect in heterometallic 3d-4f coordination clusters with high azide : metal ratios

Article (Accepted Version)

Journal Name

COMMUNICATION

SMM Behaviour and Magnetocaloric Effect in Heterometallic 3*d*-4*f* Coordination Clusters with High Azide:Metal Ratios

Received 00th January 20xx,
Accepted 00th January 20xx

DOI: 10.1039/x0xx00000x

www.rsc.org/

Sebastian F. M. Schmidt,[a] Marcel P. Merkel,[d] George E. Kostakis,[b] Gernot Buth,[c] Christopher E. Anson[a] and Annie K. Powell [a,d]

We present the synthesis and characterization of heterometallic compounds with a very large azide to metal ratio. Their interesting structure gives rise to fascinating magnetic properties.

Azide is a fascinating ligand attracting interest due to its many applications[1] including molecular magnetism. When azide couples two paramagnetic metals in an end-to-end ($\mu_{1,3}$-N_3) fashion antiferromagnetic interactions are favoured. When it couples in an end-on way ($\mu_{1,1}$-N_3) ferromagnetic interactions dominate over a broad angle range.[2] The discovery that the magnetic interactions in azide bridged compounds are easily controlled has led to the synthesis of a wide variety of homometalic compounds ranging from discrete clusters to 3d frameworks exhibiting interesting magnetic and multiferroic properties.[3] Since a high spin ground state is a crucial component for Single Molecule Magnets (SMMs) formed from ions without strong spin orbit coupling, azide ligands have been extensively used in this field.[4] Especially in heterometallic 3d 4f compounds the use of the azido ligand's end-on bridging mode is attractive because it is a controlled way to induce ferromagnetic interactions between the transition metals.[4 f-h] These kind of ferromagnetic interactions in 3d 4f compounds are not only attractive in Single Molecule Magnets but also in magnetic coolers, where a high spin ground state drives higher entropy changes in adiabatic cooling processes.[5] However, the synthesis of heterometallic coordination compounds containing bridging azide is tricky because the chelating bridging ligands used in these compounds are in competition with non-chelating azide anions, often resulting in compounds with terminal azido ligands. In order to achieve compounds with a high azide content and, if possible, including bridging azides, we used stable homoleptic azidometalates of iron and manganese in combination with lanthanide salts and aminoalcohols. We were able to obtain two structurally different coordination compounds with a very high metal to azide ratio: $TBA_3[Fe_3Gd_2(N_3)_{15}(OH)_3(tipaH_3)_2]$ **1** (5:15) (TBA = Tetrabutylammonium and $tipaH_3$ = triisopropanolamin) and $TBA_2[Mn_4Dy_2(teaH)_4(N_3)_{12}]$ ($teaH_3$ = triethanolamin) (6:12). Indeed compound **1** has the highest azide content in a discrete cluster seen so far.[6]

Compound **1** crystallises in the triclinic space group $P\bar{1}$ with Z = 2. The crystal structure consists of the anionic coordination cluster $[Fe_3Gd_2(\mu_3\text{-}OH)_3(\mu\text{-}N_3)_4(N_3)_{11}(tipaH_3)_2]^{3-}$ surrounded by three tetrabutyl ammonium cations. The cluster core can be considered as three $Gd_2Fe(\mu_3\text{-}OH)$ triangles sharing their Gd··Gd edges to give a Fe_3Gd_2 trigonal-bipyramidal core with the two Gd^{III} ions at the apices and the three Fe^{III} ions describing the central triangular plane. Within the $Gd_2Fe(\mu_3\text{-}OH)$ triangles, the Fe-O and Gd-O bond lengths lie in the range 2.0659(17)-2.0857(17) Å and 2.3984(18)-2.4882(17) Å, while the Gd-O-Gd and Gd-O-Fe angles are 96.71(6)-97.75(6)° and 108.80(7)-124.71(8)°, respectively. Each Gd is chelated by a neutral ($tipaH_3$) ligand. The $tipaH_3$ ligand was racemic, but every molecule demonstrates a chiral separation with an S,S,S and a R,R,R configuration at each of the Gd^{III} centres. This $\{Fe_3Gd_2(\mu_3\text{-}OH)_3(tipaH_3)_2\}$ core approximates to C_{3h} symmetry, but broken by the azide ligands. Each Fe centre is ligated by five azides resulting in slightly distorted octahedral N5O coordination environments and each bridge to one of the Gd centres. Six such bridges would maintain the C_{3h} symmetry, but would require each Gd to be ten-coordinate. Three of the azide bridges (involving N(11), N(21) and N(41)) have similar geometries, with Fe-N 2.048(2)-2.145(2) Å, Gd-N 2.525(2)-2,597(2) Å and Fe-N-Gd 102.93(9)-106.79(9)°. Gd(1)-N(31) is

[a] *Institut für Anorganische Chemie, Karlsruher Institute of Technology (KIT), Engesserstr. 15, D-76131 Karlsruhe, Germany. E-mail: annie.powell@kit.edu; Fax: +49 721 608 8142; Tel: +49 721 608 2135*
[b] *Department of Chemistry, University of Sussex, School of Life Sciences, Arrundel Building 305, BN1 9QJ, UK*
[c] *Institute for Photon Science and Synchrotron Radiation (IPS), Karlsruher Institute of Technology (KIT), Herrmann-von-Helmholtz-Platz 1, 76344 Eggenstein-Leopoldshafen, Germany*
[d] *Institut für Nanotechnologie, Karlsruher Institute of Technology (KIT), Postfach 3640, D-76021 Karlsruhe, Germany*
Electronic Supplementary Information (ESI) available: [experimental details, crystallographic tables and additional magnetic measurements]. See DOI: 10.1039/x0xx00000x

longer at 2.853(3) Å and this bond is shown dashed in Figure 1; other Gd··N distances are all over 3 Å. The hydroxyl groups of the organic ligands each form a hydrogen bond to a non-bridging azide ligand, adding stability to the structure.

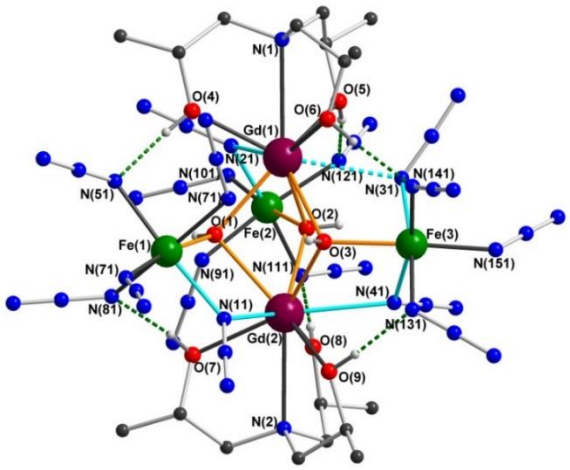

Figure 1: Structure of the cluster anion in **1** (left). Organic H atoms omitted for clarity, bonds to bridging oxygens highlighted in orange, bonds to bridging azides shown as cyan, hydrogen bonds as green dashed lines.

Compound **2** crystallises in the monoclinic space group $P2_1/c$ with Z = 2; the centrosymmetric dianionic cluster $[Mn^{III}_4Dy^{III}_2(teaH)_4(\mu\text{-}N_3)_2(N_3)_{10}]^{2-}$ (Figure 2) is charge-balanced by two tetrabutylammonium cations.

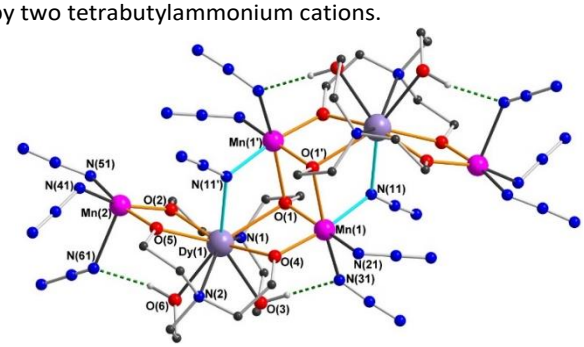

Figure 2: Structure of the cluster anion in 2. Organic H atoms omitted for clarity, bonds to bridging oxygens highlighted in orange, bonds to bridging azides shown as cyan, hydrogen bonds as green dashed lines.

Dy(1) is chelated by two doubly-deprotonated $(teaH)^{2-}$ ligands. One deprotonated oxygen from each of these ligands, O(2) and O(5), forms a double alkoxo bridge to Mn(2). Of the other two deprotonated oxygens, O(4) bridges between Dy(1) and Mn(1), while O(1) forms a triple-bridge between Dy(1), Mn(1) and Mn(1'). The azide nitrogen N(11) forms a further end-on bridge between Mn(1) and Dy(1'), and together with its inversion equivalent N(11') completes the Mn_2Dy_2 "butterfly" inner core. The coordination environment of Mn(1) is completed by two terminal azide ligands, giving a distorted N3O3 octahedral geometry, in which the elongated Jahn-Teller axis of the Mn^{III} is defined by N(31) and O(1'). Mn(2) has a square-pyramidal N3O2 geometry with three terminal azides and the bridging oxygens occupying the basal sites. The coordination geometry of Dy(1) is best described as a capped square antiprism, with N(2) capping the distorted square defined by O(3), O(4), O(5) and O(6) (Figure S2). Magnetic properties of 1

Solid state direct current (dc) magnetic susceptibility data on dried analytically pure samples of **1** and **2** were collected between 1.8 – 300 K in an applied field of 0.1 T (Figure 3, Table 1, Figure S3 – S6).

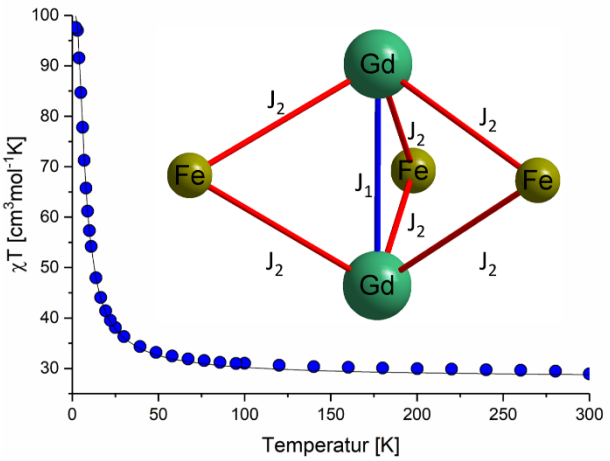

Figure 3 χT vs T of **2** at an applied field of 0,1 T. The solid line is a fit of the data. Inset: Spin model used for the fit

For both complexes the experimental values at 300 K are close to the theoretical values for non-interacting metal ions of 29.3 cm^3 K mol^{-1} for **1** and 42.42 cm^3 mol^{-1} K for **2**. In the case of **1** the χT product is almost constant down to 50 K, below which it rises to a value of 97.6 cm^3 mol^{-1} K at 2 K, which can be compared to the theoretical value for a fully ferromagnetic S = 29/2 ground state of 112.3 cm^3 mol^{-1} K, indicating that most or all of the interactions between the spin centres are ferromagnetic. In order to quantify this behaviour a Heisenberg type spin Hamiltonian was employed for the fit of the data with PHI.[7] To avoid overparametrisation the six J_{FeGd} are constrained to be equal:

$$\hat{H} = -2(\hat{S}_{Gd}\, J_1\, \hat{S}_{Gd}) - 2 * 6(\hat{S}_{Fe}\, J_2\, \hat{S}_{Gd}) + g_{Gd}\mu_B \hat{S}_{Gd} + g_{Fe}\mu_B \hat{S}_{Fe}$$

Table 1 Summary of the magnetic data of **1**

χT(295 K)	29.3 cm^3 K mol^{-1}
M (7 T, 2 K)	28.3 μ_B
g_{Fe}	1.94
J_1	0.011 cm^{-1} (0.016 K)
J_2	0.267 cm^{-1} (0.38 K)

In the case of **2** the χT value drops slightly to a value of 38.28 cm^3 mol^{-1} K at 48 K after which it drops more rapidly to a value of 13.56 cm^3 mol^{-1} K at 1.8 K. This behaviour is likely to result from a combination of the depopulation of excited states and weak antiferromagnetic interactions. This is typical for the $Mn^{III}_2Dy^{III}_2$ butterfly motif at the centre of the structure. Studies of the magnetisation (M) of **1** at different fields and temperatures gives a saturation value of 28.2 μ_B at 2 K and 7 T consistent with the maximum spin ground state of S = 29/2

(Figure S3). This large value makes **1** a possible candidate for use in magnetic cooling devices. The magnetocaloric effect (MCE) can be evaluated from the magnetisation data (Figure 4) using the Maxwell equation to relate the entropy change with changes in magnetisation:

$$\Delta S(T, \Delta H) = \int \left[\frac{\delta M\ (T,H)}{\delta T}\right]_H dH$$

The maximum entropy change is 21.1 J Kg^{-1} K^{-1} at a field change of 7 T and a temperature of 6 K.

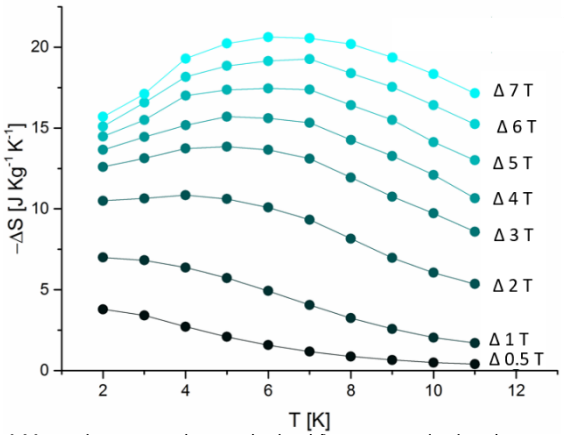

Figure 4 Magnetic entropy change obtained from magnetization data at various field changes and temperatures

The potential maximum entropy change is 34.4 J Kg^{-1} K^{-1}. The difference between the calculated and observed value might be the result of a small but significant anisotropy of the Fe^{III} ions.[8f] Since the core-structure contains a ferromagnetically coupled Gd_2 unit it is instructive to compare the MCE of **1** with that of other compounds carrying such a unit.[8] Compared to the maximum entropy change seen in Gd dinuclear compounds the value is in the low range and clearly surpassed by e.g. $Gd_2(OAc)_6(H_2O)_4$ which has an entropy change value of 66.5 J Kg^{-1} K^{-1}.[8c] However, an advantage of compound **1** is the fact that it reaches its maximum entropy change already at 6 K, compared to a T_{max} of about 1 K for the pure Gd compounds. This is related to the strength of the Gd-Fe coupling which is essentially twenty times larger than the Gd-Gd interactions. Thus 3d-4f coupling offers the means for tuning T_{max} and therefore the attainable liquification temperature for cryogens.

In order to probe the anisotropic nature of **2** we performed alternating current (ac) susceptibility measurements. These show temperature and frequency dependent signal between 1 to 1500 Hz and 1.8 to 3.8 K. (Figure 5) A striking feature of these plots is the onset of a second signal at low temperatures, but with no clear maxima in the accessible frequency range. To determine the height of the energy barrier against the reversal of magnetization the positions of the frequency dependent maxima were fitted to an Arrhenius law (Figure S6). Giving an energy barrier of 43.8 K with a pre-exponential relaxation factor of $1.47*10^{-10}$ s. There is clearly more than one relaxation process, as seen from the Cole-Cole plot resulting from the in-phase vs. out-of-phase susceptibility, where two relaxation processes are obvious, but the second relaxation process does not achieve a full semicircle. Between 2.2 and 2.4 K both relaxation processes can be accessed.

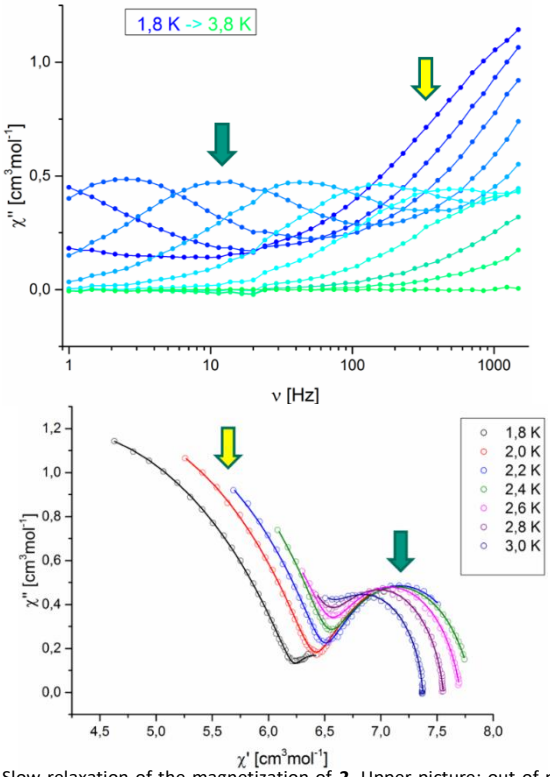

Figure 5 Slow relaxation of the magnetization of **2**. Upper picture: out-of-phase susceptibility χ'' vs frequency ν at different temperatures. Lower picture: Cole-Cole plot of **2**. In both pictures the relaxation process occurring at low temperatures is marked with a yellow arrow and the relaxation process occurring at high temperatures is marked with a green arrow.

Since they show a frequency dependent behaviour, QTM is an unlikely source for the second relaxation process, reminiscent of the situation for $Co^{II}_2Dy^{III}_2$ butterflies.[9] Due to the strong spin orbit coupling of the Dy^{III} ions a fit of the magnetic properties is impossible. However, the weak magnetic interactions between the 3d and 4f metal ions allow for an analysis of different parts of the structure. The strongest interactions are expected to be found in the central $\{Mn^{III}_2\}$ unit. Their Jahn-Teller axis are perpendicular to the bridging plane so that mostly dx^2-y^2 orbitals take part in the coupling of the two ions. Jones et al. defined this kind of bridging as a type I bridge for which antiferromagnetic interactions between J = -8.2 cm-1 and J = -15.5 cm-1 are to be expected.[10] This $\{Mn_2\}$ unit is part of the $\{Mn_2Dy_2\}$ butterfly core. In the literature several $Mn^{III}_2Dy_2$ structures with a similar motif are known,[11] however the interactions between the spin centres differ greatly from strong antiferromagnetic interactions[11d,e] to ferromagnetic interactions[11c] with only one compound showing slow relaxation of the magnetisation with an energy barrier of 29 K.[11 d] Thus it is more likely that the high temperature regime relaxation results from the whole molecule whereas at low temperature individual ion processes may dominate.

Conclusions

In conclusion we present two new heterometallic coordination compounds containing a very high azide to metal ratio. These compounds were synthesised from the reaction of homoleptic azidometallate precursors with tripodal ligands and lanthanide salts. In both compounds the interactions through the bridging azides cause interesting magnetic effects. In compound **1**, with a Fe_3Gd_2 core with 15 coordinating azides, the interactions between the metal centers are ferromagnetic. This leads to a high spin ground state of S = 29/2. This high spin ground state can be used in devices for magnetic cooling. There is a high maximum entropy change of 21.1 J Kg^{-1} K^{-1} at a field change of 7 T and a temperature of 6 K. On the other hand the $Mn^{III}_4Dy_2$ compound proves to be the first example of a Mn^{III}-Dy SMM showing more than one relaxation processes.

Conflict of Interest

There are no Conflicts to declare.

Acknowledgements

The work was supported in part by the Deutsche Forschungsgemeinschaft through the projects FOR1154 „Towards Molecular Spintronics“ and INST 35 / 1085-1 FUGG and TR-SFB 88 “3MET”.

Notes and references

1 (a) W. P. Fehlhammer and W. Beck, *Z. Anorg. Allg. Chem.*, 2013, **639**, 1053–1082. (b) P. Portius and M. Davis, *Coord. Chem. Rev.*, 2013, **257**, 1011–1025.

2 (a) M. A. Aebersold, O. Plantevin, L. Pardi, O. Kahn, P. Bergerat, I. Von Seggern, F. Tuczek, L. Öhrström, A. Grand and E. Lelievre-Berna, *J. Am. Chem. Soc.*, 1998, **120**, 5238–5245. (b) M.-F. Charlot, O. Kahn, M. Chaillet and C. Larrieu, *J. Am. Chem. Soc.*, 1986, **108**, 2574–2581.

3 (a) M. A. S. Goher, J. Cano, Y. Journaux, M. A. M. Abu-youssef, F. A. Mautner, A. Escuer and R. Vicente, *Chem. Eur. J.*, 2000, **6**, 778–784. (b) T. Liu, Y. Zhang, Z. Wang and S. Gao, *Inorg. Chem.*, 2006, **45**, 2782–2784. (c) G. De Munno, T. Poerio, G. Viau, M. Julve and F. Lloret, *Angew. Chem. Int. Ed. Engl.*, 1997, **36**, 1459–1461. (d) X. Liu, P. Cen, H. Li, H. Ke, S. Zhang, Q. Wei, G. Xie, S. Chen and S. Gao, *Inorg. Chem.*, 2014, **53**, 8088–8097. (e) J. Suarez-Varela, I. B. Maimoun and E. Colacio, *Dalt. Trans.*, 2004, 3938–3940. (f) X.-H. Zhao, X.-C. Huang, S.-L. Zhang, D. Shao, H.-Y. Wei and X.-Y. Wang, *J. Am. Chem. Soc.*, 2013, **135**, 16006–16009. (g) X. Liu, X. Qu, S. Zhang, H. Ke, Q. Yang, Q. Shi, Q. Wei, G. Xie and S. Chen, *Inorg. Chem.*, 2015, **54**, 11520–11525. (h) Y. Z. Zhang, H.-Y. Wei, F. Pan, Z.-M. Wang, Z.-D. Chen and S. Gao, *Angew. Chem. Int. Ed. Engl.*, 2005, **44**, 5841–5846. (i) L. C. Gómez-Aguirre, B. Pato-Doldán, A. Stroppa, L. M. Yang, T. Frauenheim, J. Mira, S. Yáñez-Vilar, R. Artiaga, S. Castro-García, M. Sánchez-Andújar and M. A. Señarís-Rodríguez, *Chem. Eur. J.*, 2016, **22**, 7863–7870.

4 (a) A. M. Ako, V. Mereacre, R. Clérac, W. Wernsdorfer, I. J. Hewitt, C. E. Anson and A. K. Powell, *Chem. Commun.* , 2009, 544–546. (b) A. M. Ako, I. J. Hewitt, V. Mereacre, R. Clerac, W. Wernsdorfer, C. E. Anson and A. K. Powell, *Angew. Chem. Int. Ed. Engl.*, 2006, **45**, 4926–4929. (c) F. Klöwer, Y. Lan, J. Nehrkorn, O. Waldmann, C. E. Anson and A. K. Powell, *Chem. Eur. J.*, 2009, **15**, 7413–7422. (d) C. H. Ge, A. L. Cui, Z. H. Ni, Y. B. Jiang, L. F. Zhang, J. Ribas and H. Z. Kou, *Inorg. Chem.*, 2006, **45**, 4883–4885. (e) D. Schray, G. Abbas, Y. Lan, V. Mereacre, A. Sundt, J. Dreiser, O. Waldmann, G. E. Kostakis, C. E. Anson and A. K. Powell, *Angew. Chem. Int. Ed. Engl.*, 2010, **49**, 5185–8. (f) S. Schmidt, D. Prodius, G. Novitchi, V. Mereacre, G. E. Kostakis and A. K. Powell, *Chem. Commun.* , 2012, **48**, 9825–9827. (g) S. Schmidt, D. Prodius, V. Mereacre, G. E. Kostakis and A. K. Powell, *Chem. Commun.* , 2013, **49**, 1696–1698. (h) S. F. M. Schmidt, C. Koo, V. Mereacre, J. Park, D. W. Heermann, V. Kataev, C. E. Anson, D. Prodius, G. Novitchi, R. Klingeler and A. K. Powell, *Inorg. Chem.*, 2017, **56**, 4796–4806.

5 (a) M. Evangelisti, in *Molecular Magnets*, eds. J. Bartolomé, F. Luis and J. F. Fernandez, Springer Berlin Heidelberg, 2014, pp. 365–387. (b) J.-L. Liu, Y.-C. Chen, F.-S. Guo and M.-L. Tong, *Coord. Chem. Rev.*, 2014, **281**, 26–49. (c) M. Evangelisti and E. K. Brechin, *Dalt. Trans.*, 2010, **39**, 4672–4676. (d) F. Luis and M. Evangelisti, in *Molecular Nanomagnets and Related Phenomena*, ed. So. Gao, Springer Berlin Heidelberg, 2014, pp. 432–460.

6 M. D. Walter, F. Weber, G. Wolmershäuser and H. Sitzmann, *Angew. Chem. Int. Ed. Engl.*, 2006, **45**, 1903–1905.

7 N. F. Chilton, R. P. Anderson, L. D. Turner, A. Soncini and K. S. Murray, *J. Comput. Chem.*, 2013, **34**, 1164–1175.

8 (a) L. Sedláková, J. Hanko, A. Orendácova, M. Orendác, C.-L. Zhou, W.-H. Zhu, B.-W. Wang, Z.-M. Wang and S. Gao, *J. Alloys Compd.*, 2009, **487**, 425–429. (c) M. Evangelisti, O. Roubeau, E. Palacios, A. Camón, T. N. Hooper, E. K. Brechin and J. J. Alonso, *Angew. Chem. Int. Ed. Engl.*, 2011, **50**, 6606–6609. (d) G. Lorusso, J. W. Sharples, E. Palacios, O. Roubeau, E. K. Brechin, R. Sessoli, A. Rossin, F. Tuna, E. J. L. McInnes, D. Collison and M. Evangelisti, *Adv. Mater.*, 2013, **25**, 4653–4656. (e) G. Lorusso, M. A. Palacios, G. S. Nichol, E. K. Brechin, O. Roubeau and M. Evangelisti, *Chem. Commun.*, 2012, **48**, 7592. (f) F. S. Guo, J. D. Leng, J. L. Liu, Z. S. Meng and M. L. Tong, *Inorg. Chem.*, 2012, **51**, 405–413. K. S. (f) Pedersen, G. Lorusso, J. J. Morales, T. Weyhermüller, S. Piligkos, S. K. Singh, D. Larsen, M. Schau-Magnussen, G. Rajaraman, M. Evangelisti and J. Bendix, Angew. Chem. Int. Ed. Engl., 2014, 53, 2394–2397.

9 (a) K. C. Mondal, A. Sundt, Y. Lan, G. E. Kostakis, O. Waldmann, L. Ungur, L. F. Chibotaru, C. E. Anson and A. K. Powell, *Angew. Chem.*, 2012, **124**, 7668–7672. (b) Y. Peng, V. Mereacre, C. E. Anson and A. K. Powell, *Dalt. Trans.*, 2017, **46**, 5337–5343. (c) X.-L. Li, F.-Y. Min, C. Wang, S. Lin, Z. Liu and J. Tang, *Inorg. Chem.*, 2015, **54**, 4337–4344.

10 N. Berg, T. Rajeshkumar, S. M. Taylor, E. K. Brechin, G. Rajaraman and L. F. Jones, *Chem. Eur. J.*, 2012, **18**, 5906–5918.

11 (a) C. Papatriantafyllopoulou, K. A. Abboud and G. Christou, *Inorg. Chem.*, 2011, **50**, 8959–8966. (b) A. Mishra, W. Wernsdorfer, S. Parsons, G. Christou and E. K. Brechin, *Chem. Commun.*, 2005, 2086. (c) G. P. Guedes, S. Soriano, L. A. Mercante, N. L. Speziali, M. A. Novak, M. Andruh and M. G. F. Vaz, *Inorg. Chem.*, 2013, **52**, 8309–8311. (d) E. Moreno Pineda, N. F. Chilton, F. Tuna, R. E. P. Winpenny and E. J. L. McInnes, *Inorg. Chem.*, 2015, **54**, 5930–5941. (e) C. Benelli, M. Murrie, S. Parsons and R. E. P. Winpenny, *J. Chem. Soc. Dalt. Trans.*, 1999, 4125–4126. (f) L. Sun, H. Chen, C. Ma and C. Chen, *Inorg. Chem.*, 2016, **70**, 132–135. (g) V. Mereacre, Y. Lan, R. Clérac, A. M. Ako, I. J. Hewitt, W. Wernsdorfer, G. Buth, C. E. Anson and A. K. Powell, *Inorg. Chem.*, 2010, **49**, 5293–5302.

